OPTICAL FIBER TECHNOLOGY **4,** 204–214 (1998)
ARTICLE NO. OF980248

Invited Paper

Highly Nonlinear Dispersion-Shifted Fibers and Their Application to Broadband Wavelength Converter

M. Onishi, T. Okuno, T. Kashiwada, S. Ishikawa, N. Akasaka, and M. Nishimura

Sumitomo Electric Industries, Ltd., 1, Taya-cho, Sakae-ku, Yokohama 244-8588, Japan

Received December 10, 1997

Highly nonlinear dispersion-shifted fibers were designed and fabricated for efficient nonlinear effect generation. High-concentration GeO_2-doped core and fluorine-doped cladding were employed in this study, and the fabricated fiber successfully realized a high nonlinear coefficient of 20.4 W^{-1} km^{-1} and a low attenuation of 0.51 dB/km. Using the fabricated fiber, four-wave mixing (FWM) generation was demonstrated aiming at its application to wavelength conversion, and its efficiency, which was defined as the ratio of the FWM product to the input signal power, was dramatically improved to about 60 times higher than that with the conventional dispersion-shifted fibers. The enhanced conversion efficiency allows the required fiber length to be shortened, and this is also beneficial to reduction of the overall zero dispersion wavelength fluctuation, which contributes to broadband wavelength conversion. The fabricated fiber shorter than 500 m exhibited efficient generation of FWM, and a nearly constant wavelength conversion efficiency over 20 nm, which covers most of the erbium-doped fiber amplifier gain bandwidth, was successfully demonstrated. © 1998 Academic Press

1. INTRODUCTION

Four-wave mixing (FWM) is one of the interesting nonlinear effects observed in optical fibers. It has been studied for various applications such as wavelength conversion [1], optical switching [2], high-speed signal demultiplexing [3], and dispersion compensation using phase-conjugated signals [4]. Especially, the wavelength-conversion is quite attractive in the field of optical cross-connection for

1068-5200/98 $25.00

future photonic networks. There have been several reports on the wavelength conversion using the FWM in the conventional dispersion-shifted fiber (DSF) [5]. However, a fiber length greater than 10 km is typically required for practical applications because of its low nonlinearity and its narrow bandwidth (< 5 nm), which is attributed to fluctuation of the zero dispersion wavelength (λ_0) along the fiber length and which has also been pointed to as a drawback in comparison with semiconductor optical amplifiers (SOAs) as wavelength converters [6]. On the other hand, wavelength conversion using FWM in optical fibers can realize low noise and simultaneous conversion of wavelength-multiplexed signals, while SOAs intrinsically exhibit relatively large noise originating from amplified spontaneous emission (ASE), and it is also difficult for SOAs to convert the multiple wavelengths simultaneously. DSFs with high nonlinearity therefore have been of great interest [7, 8].

In this paper, highly nonlinear dispersion-shifted fibers (HNL-DSFs) are designed and fabricated, and an enhanced nonlinear coefficient (γ) of 20.4 W^{-1} km^{-1}, which is 7.6 times higher than that of conventional DSFs, is realized while maintaining a low attenuation of 0.51 dB/km at 1550 nm. Additionally, the fabricated DSF shorter than 500 m efficiently generates the FWM product, and broadband wavelength conversion which covers a bandwidth of more than 20 nm is demonstrated. Polarization maintaining HNL-DSFs and a fully engineered wavelength converter module will also be discussed.

2. FIBER DESIGN AND FABRICATION

The refractive index profile used in our study is shown in Fig. 1. Δ^+ and Δ^- indicate the refractive index difference between the center of the core or the cladding and the pure silica level, respectively. The core is germanium-doped and has a graded index profile, and the cladding is doped with fluorine in order to obtain low attenuation with constant $\Delta^- = 0.35\%$ [9]. Using this refractive index profile, the chromatic dispersion, the mode field diameter (MFD), and the LP_{11} cut off wavelength were calculated by the finite element method (FEM) [10]. Figure 2 shows the MFD, chromatic dispersion slope at 1550 nm, and LP_{11} cutoff as a

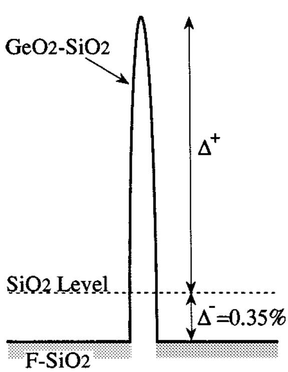

FIG. 1. Refractive index profile used in this study.

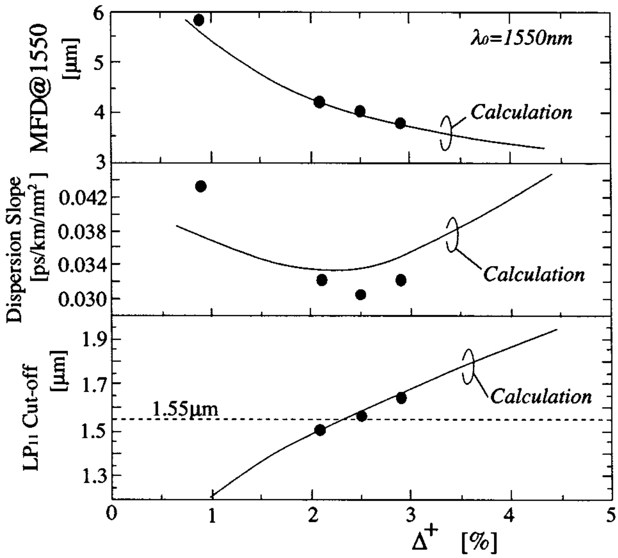

FIG. 2. MFD, chromatic dispersion slope, and LP_{11} cutoff at 1550 nm as a function of Δ^+.

function of Δ^+, while the core diameter is always adjusted so as to obtain λ_0 of 1550 nm. With increasing Δ^+, the MFD decreases, and highly nonlinear DSFs with an effective core area (A_{eff}) smaller than 15 μm^2 (MFD < 4.3 μm) are expected when Δ^+ is larger than 2.0%. On the other hand, the dispersion slope is minimized to +0.034 ps/km/nm^2 when Δ^+ is around 2.3%. The small dispersion slope is believed to be beneficial to broadband FWM generation. Additionally, although the LP_{11} cutoff is longer than 1550 nm if Δ^+ is larger than 2.3%, this shall not cause a problem, because higher order modes are sufficiently eliminated when fibers are wound into small coils in the practical applications [11].

We have fabricated HNL-DSFs with Δ^+ of 2.1, 2.5, and 2.9% by the vapor-phase axial deposition (VAD) method. The measurement results of the fabricated fibers are also plotted in Fig. 2, indicating a good agreement with the calculations. Fiber parameters and properties of the fabricated fibers are summarized in Table 1. In particular, Fiber A exhibited γ of 20.4 $W^{-1}km^{-1}$, which is 7.6 times larger than that for the conventional DSFs. Attenuation and dispersion spectra of Fiber A are shown in Fig. 3. The zero dispersion wavelength (λ_0) was precisely tuned to 1550 nm, and the dispersion slope at λ_0 was as small as +0.032 ps/km/nm^2. Attenuation at 1550 nm was as low as 0.51 dB/km in spite of the high concentration of GeO_2.

3. EFFICIENCY OF FWM GENERATION

Figure 4 shows the calculated iso-conversion efficiency diagram against γ and the fiber length. In our study, the conversion efficiency is defined as the ratio of the FWM product power to the input probe power. The output power of the FWM

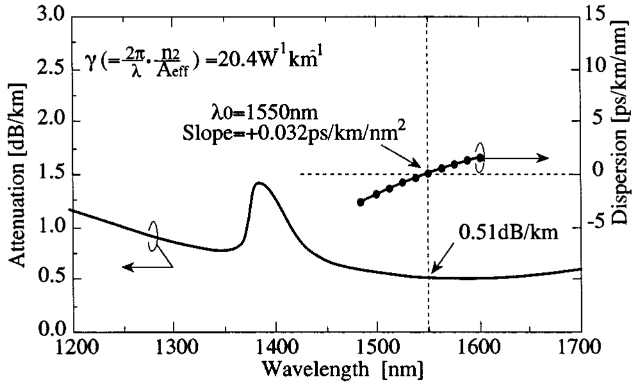

FIG. 3. Attenuation and dispersion spectra of Fiber A with a γ of 20.4 W^{-1} km^{-1}.

product is calculated by equations [12]

$$P_{\rm FWM}(L) = \gamma^2 \cdot \left[P_{\rm pump}(0)\right]^2 \cdot P_{\rm probe}(0) \cdot \exp(-\alpha L) \cdot L_{\rm eff}^2 \cdot \eta \tag{1}$$

$$L_{\rm eff} = \frac{1-\exp(-\alpha L)}{\alpha} \tag{2}$$

$$\eta = \frac{\alpha^2}{\alpha^2 + (\Delta\beta)^2}\left[1 + \frac{4e^{-\alpha L}\sin(\Delta\beta L/2)}{\{1-\exp(-\alpha L)\}^2}\right] \tag{3}$$

$$\Delta\beta = -2c\lambda_0^4\pi\frac{dD}{d\lambda}\left(\frac{1}{\lambda_{\rm pump}} - \frac{1}{\lambda_{\rm probe}}\right)^2 \times \left(\frac{1}{\lambda_{\rm pump}} - \frac{1}{\lambda_0}\right), \tag{4}$$

where $P_{\rm pump}$ is the pumping power, $P_{\rm probe}$ is the probe power, α is the fiber loss, L is the fiber length, and $dD/d\lambda$ is the dispersion slope.

TABLE 1
Fiber Parameters and Properties of Fabricated Fibers

Fiber	Δ^+[%]	Δ^-[%]	Attenuation [dB/km]	MFD [μm]	$A_{\rm eff}$ [μm^2]	γ [1/W/km]	λ_0 [nm]	Slope [ps/km/nm^2]	λ_c [μm]
A	2.9	0.35	0.51	3.8	10.7	20.4	1550	0.032	1.63
B	2.1	0.35	0.34	4.2	13.8	13.2	1551	0.032	1.50
Conv. DSF	(Dual shape core)		0.20	8.0	50.0	2.7	1547	0.066	1.07

Note. ($\gamma = (2\pi/\lambda)\cdot(n_2/A_{\rm eff})$).

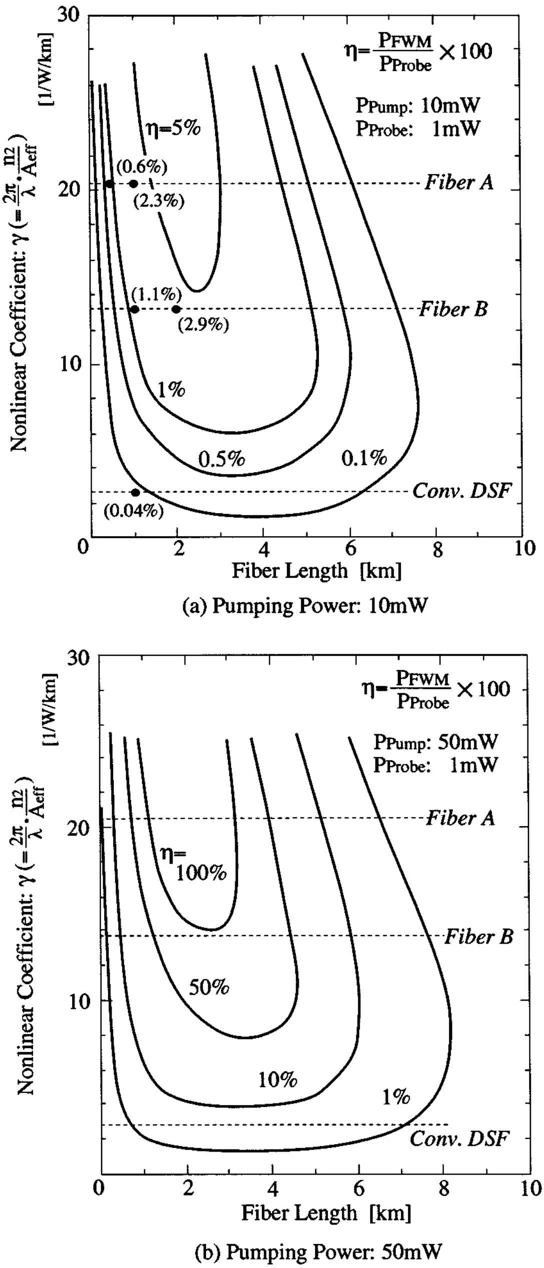

FIG. 4. Iso-conversion efficiency (η) diagram against fiber nonlinearity coefficient (γ) and fiber length. (a) Pumping power, 10 mW. (b) Pumping power, 50 mW.

In our calculations, actual fiber losses measured for the fabricated fibers were used, and the pump wavelength was assumed to be equal to λ_0. Other nonlinear effects such as stimulated Brillouin scattering were not taken into account. As shown in Fig. 4, the conversion efficiency increases dramatically with increasing γ, while the fiber length giving the maximum conversion efficiency becomes shorter,

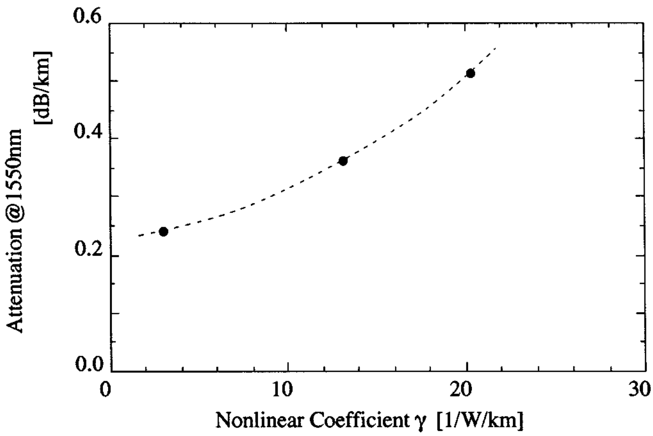

FIG. 5. Attenuation of fabricated fibers as a function of nonlinear coefficient (γ).

because fiber loss is deteriorated when γ is increased by enhancing a doping level of GeO_2 as shown in Fig. 5. It is predicted from Fig. 4b that HNL-DSFs with γ larger than 16 $W^{-1}km^{-1}$ enable transparent conversion ($\eta = 100\%$) with the fiber length shorter than 3 km and 50 mW pump power. The conversion efficiency of Fibers A and B and the conventional DSF was experimentally evaluated by using the setup illustrated in Fig. 6. Results are plotted in Fig. 4a, and they are in good agreement with the calculation. In Fiber A, the conversion efficiency of 2.3% was achieved with only 1 km of the fiber and only 10 mW pump power. This is 58 times more efficient than the efficiency measured under the same conditions using conventional DSF.

4. WAVELENGTH CONVERSION BANDWIDTH

In order to realize broadband wavelength conversion, phase matching between the pump and the signals is required in general. This can be achieved by setting the pumping wavelength to λ_0 of the fiber; however, λ_0 fluctuates to some degree in the overall length of the fiber, and this may deteriorate the conversion efficiency in a wide wavelength band. In this regard, the shorter fiber length required for the HNL-DSF with enhanced γ should also be beneficial. Figure 7 shows the measured dependence of the FWM output power upon the probe wavelength when 500

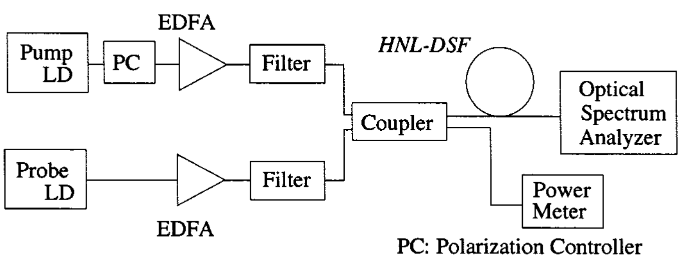

FIG. 6. Experimental setup for FWM efficiency and bandwidth evaluation.

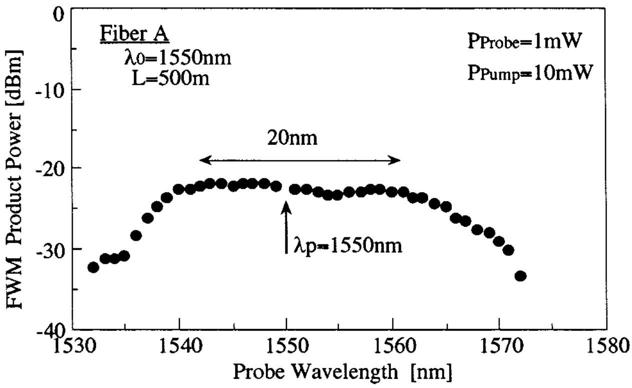

FIG. 7. Probe light wavelength dependence of generated FWM output power for Fiber A with a γ of 20.4 W^{-1} km^{-1}.

m of Fiber A was pumped at λ_0. Input pump and probe powers were 10 and 1 mW, respectively. A fairly flattened spectrum of the conversion efficiency over a bandwidth more than 20 nm was successfully achieved.

5. POLARIZATION MAINTAINING HIGHLY NONLINEAR DSF

In order to realize stable and highly efficient wavelength conversion, it is important to maintain the polarization state in the overall length of the fiber, because phase matching also depends on the polarization states of the pump and the signal lights. Therefore, polarization maintaining HNL-DSF (PM-HNL-DSF) is quite attractive for future practical applications. Figure 8 shows the fiber structure, which employs the conventional polarization maintaining and absorption reducing (PANDA) structure. Fiber properties of the fabricated fiber are listed in Table 2. For 1 km of the fabricated fiber, 24 dB of crosstalk between the orthogonal

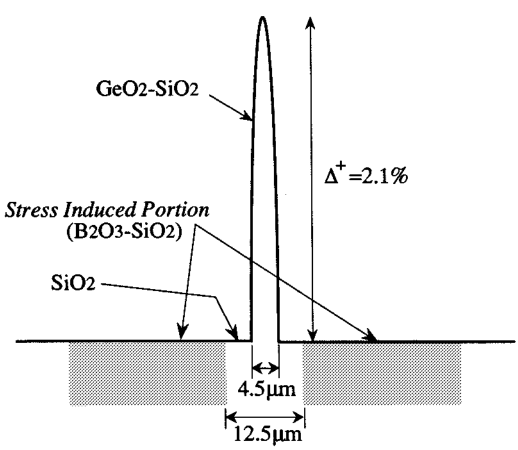

FIG. 8. Refractive index profile of fabricated PM-HNL-DSF.

TABLE 2
Fiber Properties of Fabricated PM-HNL-DSF

Attenuation [db/km]	γ [1/W/km]	λ_0 [nm]	Crosstalk (L = 1 km) [db]	MFD (∥/⊥) [μm]	λ_c (∥/⊥) [μm]
0.65	11	1583	24	4.4/4.7	1.46/1.35

Note. ∥: Parallel to the stress induced portions axis. ⊥ : Perpendicular to the stress induced portions axis.

propagation modes was successfully realized. The nonlinear coefficient γ of the fiber was 11 $W^{-1}km^{-1}$, which is about 4 times larger than those for conventional DSFs. The γ was slightly degraded in comparison with Fibers A and B, because Δ^+ was relatively low (2.1%) and the pure silica cladding was employed. In addition, λ_0 of the fiber was slightly off the erbium-doped fiber amplifier (EDFA) gain bandwidth in this example, but this can be adjusted easily by tuning the core parameters.

6. WAVELENGTH CONVERTER MODULE

A compactly packaged four-wave-mixing-based wavelength converter has been developed by utilizing the fabricated highly nonlinear DSF. Due to its high numerical aperture, the highly nonlinear DSF is very insensitive to bending, showing almost no excessive loss even with a 20-mm bending diameter. Figure 9 shows the configuration of the developed wavelength converter module. An erbium-doped fiber ring laser with a tunable band pass filter is used as a pump light source with CW output power over 10 dBm. Output light from this laser is

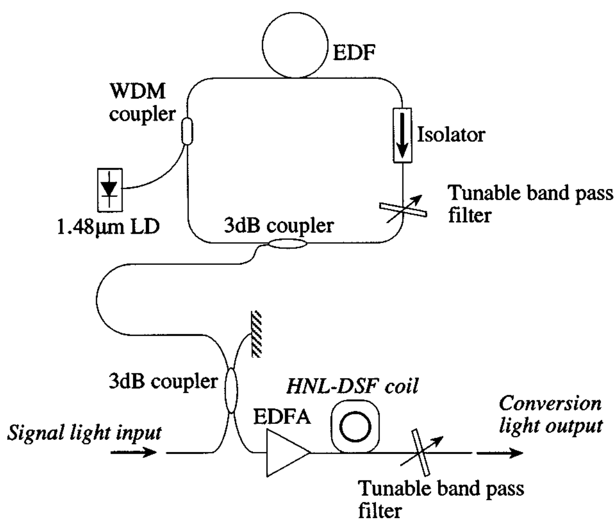

FIG. 9. Configuration of the wavelength convertor module.

multiplexed with the signal light through a 3-dB coupler. Then they are amplified by a single-LD-pumped EDFA and launched into a HNL-DSF coil. The conversion light generated in the HNL-DSF is selected by another tunable band pass filter.

Figure 10 shows the appearance of this module, whose package sizes are $165 \times 180 \times 20$ mm. The module contains all the optical components (the ring laser, the EDFA, the HNL-DSF coil, etc.) and the electronics necessary for driving pump lasers. The HNL-DSF used in this module has the same fiber parameters as those of Fiber A, but the cladding and the coating diameters have been reduced to 100 and 150 μm, respectively, because it is essential to make the fiber coil as small as possible in order to miniaturize the module. Five hundred meters of the fiber could be wound on a small bobbin having an outer diameter of 60 mm and a height of 7 mm (shown in an inset to Fig. 10). No loss increase due to coiling has been observed. Total polarization mode dispersion of this coil is only 0.26 ps.

Figure 11 shows the conversion efficiency of the module as a function of the signal wavelength observed when the pump wavelength is tuned to λ_0 of the HNL-DSF. The overall conversion efficiency higher than -15 dB has been achieved for a wavelength range from 1540 to 1556 nm when the input signal power is -2.2 dBm.

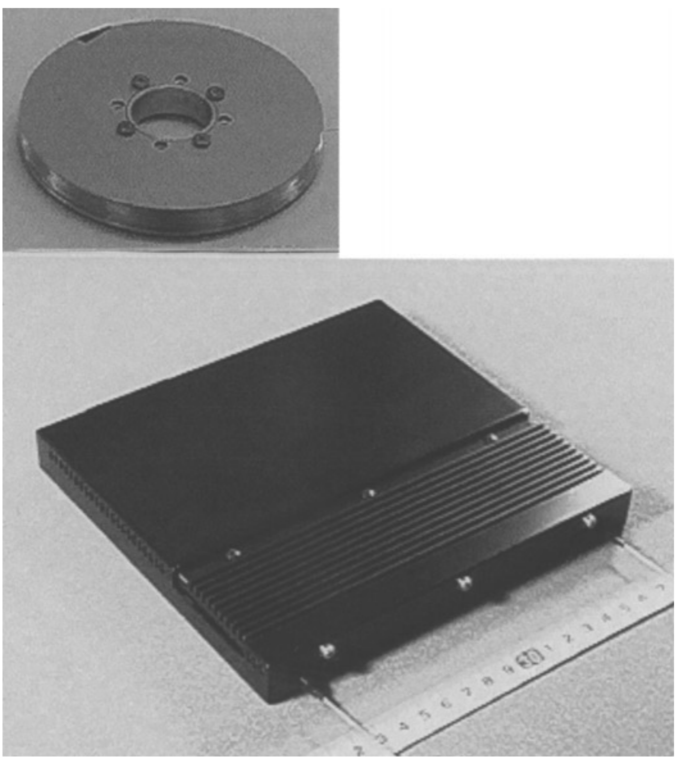

FIG. 10. The appearance of the developed wavelength converter module. Inset shows the HNL-DSF coil used in this module.

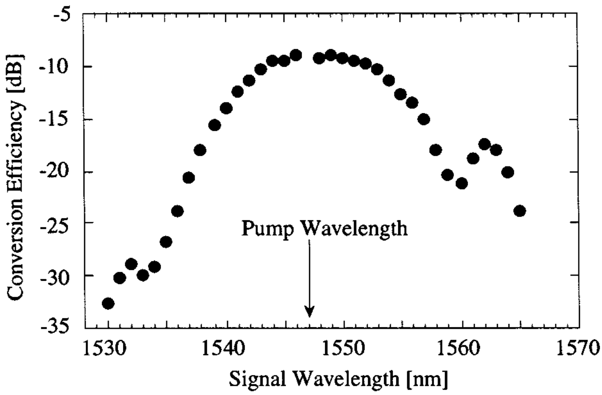

FIG. 11. Overall signal conversion efficiency of the module measured as a function of the signal wavelength.

7. CONCLUSION

We have designed and fabricated HNL-DSFs with γ larger than 20 $W^{-1}km^{-1}$ while maintaining a low loss of 0.51 dB/km. Only 500 m of the fabricated fiber successfully realized broadband wavelength conversion covering most of the EDFA gain bandwidth, and a flattened conversion efficiency spectrum over 20 nm was demonstrated. Additionally, PM-HNL-DSF with PANDA structure was fabricated, and a crosstalk of 24 dB was realized for 1 km of the fiber. Furthermore, the fabricated HNL-DSF was utilized to develop the compact wavelength converter module, which exhibited high efficiency and broad conversion bandwidth performances.

ACKNOWLEDGMENTS

The authors express their sincere thanks to Dr. Shigeki Watanabe of Fujitsu Laboratories Ltd. for helpful discussions.

REFERENCES

[1] K. Inoue and H. Toba, “Wavelength conversion experiment using fiber four-wave mixing,” *IEEE Photon. Technol. Lett.*, vol. 4, no. 1, p. 69 (1992).

[2] D. A. Pastel, A. F. Evans, R. M. Hawk, D. A. Nolan, D. L. Weidman, P. Dasika, M. Jiang, M. N. Islam, and D. G. Moodie, “High nonlinearity, low loss fiber for 1 pJ switching of 8-ps optical pulses,” in *Proc. Optical Fiber Commun.*, Dallas, Technical Digest, vol. 6, p. 168, 1997.

[3] P. A. Andrekson, N. A. Olsson, J. R. Simpson, T. Tanbun-ek, R. A. Logan, and M. Haner, “16Gbit/s all-optical demultiplexing using four-wave mixing,” *Electron. Lett.*, vol. 27, p. 922 (1991).

[4] S. Watanabe and M. Shirasaki, “Exact compensation for both chromatic dispersion and Kerr effect in a transmission fiber using optical phase conjugation,” *J. Lightwave Technol.*, vol. 14, no. 3, p. 243 (1996).

[5] P. H. Hedekvist and P. A. Andrekson, “Fiber-based pulsed wavelength convertor with ± 11 nm range and more than 20 dB of parametric gain,” in *Proc. ECOC*, Edinburgh, vol. 2, p. 184, 1997.

[6] H. Geiger, S. Y. Set, R. I. Laming, M. J. Cole, and L. Reekie, ''Comparison of DSF- and SOA-based phase conjugators employing noise-suppressing fiber,'' in *Proc. Optical Fiber Commun.*, Dallas, Technical Digest, vol. 6, p. 150, 1997.

[7] M. J. Holmes, D. L. Williams, and R. J. Manning, ''Highly nonlinear optical fiber for all optical processing applications,'' *IEEE Photon Technol. Lett.*, vol. 7, no. 9, p. 1045 (1995).

[8] S. Sudo and H. Itoh, ''Efficient non-linear optical fibres and their applications,'' *Opt. Quantum Electron.*, vol. 22, p. 187 (1990).

[9] M. Onishi, T. Kashiwada, Y. Ishiguro, Y. Koyano, M. Nishimura, and H. Kanamori, ''High-performance dispersion-compensating fibers,'' *Fiber Integrated Opt.*, vol. 16, no. 3, p. 277 (1997).

[10] K. Okamoto, ''Comparison of calculated and measured impulse response of optical fibers,'' *Appl. Opt.*, vol. 18, no. 13, p. 2199 (1979).

[11] T. Kato, Y. Suetsugu, Y. Terasawa, and M. Nishimura, ''Design optimization of dispersion shifted fiber for WDM transmission considering length dependence of cutoff wavelength,'' in *Proc. Optoelectronics & Communications Conf.*, Makuhari, Chiba, Technical Digest, p. 160, 1996.

[12] K. Inoue, ''Four-wave mixing in an optical fiber in the zero-dispersion wavelength region,'' *J. Lightwave Technol.*, vol. 10, no. 11, p. 1553 (1992).